

MatMart: Material Reconstruction of 3D Objects via Diffusion

Xiuchao Wu^{1,3*} Pengfei Zhu^{2,3*}
 Jiangjing Lyu^{3†} Xinguo Liu¹ Jie Guo² Yanwen Guo² Weiwei Xu¹ Chengfei Lyu^{3‡}
¹Zhejiang University ²Nanjing University ³Alibaba Group



Figure 1. **Reconstructed results in single-view input:** Our method reconstructs high-quality materials across various types of objects.

Abstract

Applying diffusion models to physically-based material estimation and generation has recently gained prominence. In this paper, we propose MatMart, a novel material reconstruction framework for 3D objects, offering the following advantages. First, MatMart adopts a two-stage reconstruction, starting with accurate material prediction from inputs and followed by prior-guided material generation for unobserved views, yielding high-fidelity results. Second, by utilizing progressive inference alongside the proposed view-material cross-attention (VMCA), MatMart enables reconstruction from an arbitrary number of input images, demonstrating strong scalability and flexibility. Finally, MatMart achieves both material prediction and generation capabilities through end-to-end optimization of a single diffusion model, without relying on additional pre-trained models, thereby exhibiting enhanced stability across various types of objects. Extensive experiments demon-

strate that MatMart achieves superior performance in material reconstruction compared to existing methods.

1. Introduction

Recovering materials of a 3D object from RGB images has long been a challenge in computer vision and graphics. Previous methods reconstruct material properties through differentiable rendering [12, 16, 25, 33], which typically involves per-object optimization and requires a sufficient number of captured images, consequently leading to low efficiency and high instability. Recently, approaches leveraging diffusion models for material prediction and generation have emerged [4, 13, 14, 18, 23, 31, 46, 48], providing new perspectives for inverse material decomposition.

However, there remain challenges in building a material reconstruction framework with existing methods. First, reconstructing materials with high-fidelity requires both accurate material estimation and thorough preservation of details from the input images. Unfortunately, rich textures, es-

*Equal contribution †Project leader ‡Corresponding author.

pecially meaningful ones such as text and logos present on objects, remain difficult to faithfully reproduce with current generative models. Second, to be practical, the framework should possess scalability and be capable of handling varying numbers of input images with high-resolution. However, this is often constrained by the framework design and GPU memory. Finally, it is advisable for the framework to avoid dependencies on outputs from other pre-trained models or on the use of multiple models, as these can increase the complexity of training and deployment while potentially diminishing the stability of the method.

To address the above challenges, we propose MatMart, a diffusion-based framework for high-fidelity and scalable material reconstruction, which operates in two stages. In the first stage, MatMart accurately estimates material properties from RGB inputs and bakes the results into UV space. In the second stage, MatMart adaptively selects views based on UV texel coverage, then alternates between prior-guided generation and texture baking for occluded and unobserved regions. This two-stage reconstruction can preserve the details from inputs as much as possible and fully utilize the latest prior information for generation, ultimately achieving highly faithful material recovery. To handle the potentially diverse quantities of input images present in various cases, we adopt a progressive inference strategy for both estimation and generation. As such inference does not allow cross-view attention across all views, we propose view-material cross-attention (VMCA) to ensure multi-view consistency. With this inference strategy, our framework supports prediction and generation from arbitrary numbers of inputs and higher resolutions (Fig. 4), thereby demonstrating strong scalability. Finally, in contrast to existing approaches that involve multiple models or rely on pre-trained models, MatMart unifies material prediction and generation within a single, jointly trainable model. Such a unified architecture greatly reduces the complexity of training and deployment, while also improves the stability.

In summary, our main contributions are as follows:

- We propose a novel two-stage framework for material reconstruction. Combining progressive material prediction with prior-guided generation, our framework recovers accurate PBR materials, thereby achieving highly faithful renderings across various types of objects.
- By integrating the proposed view-material cross-attention (VMCA) into progressive inference, we achieve consistent outputs with reduced memory consumption, allowing our framework to recover materials from a single to arbitrary numbers of high-resolution inputs, thereby exhibiting strong scalability and flexibility.
- Material prediction and generation are achieved using a unified architecture that operates with a single diffusion model and allows for end-to-end optimization.

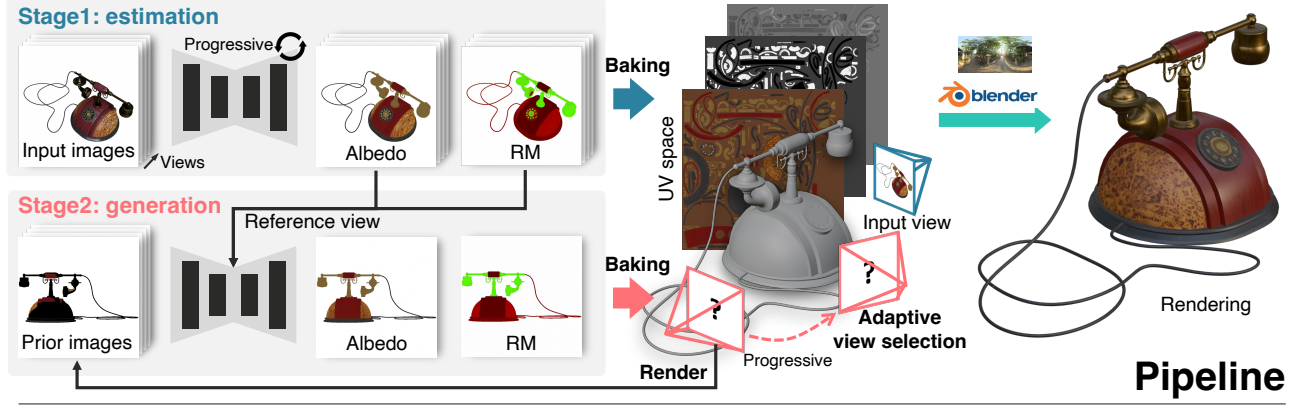
2. Related Work

2.1. Optimization-based Material Reconstruction

3D material reconstruction has been evolving for decades. The early approaches capture extensive reflectance samples using specialized devices such as gonioreflectometers [6, 32, 42] and fit BRDF parameters with high accuracy but significant acquisition cost. Recently, inverse rendering frameworks have provided end-to-end optimization of material, allowing high-quality reconstructions from image supervision alone [11, 12, 33]. Implicit representations have been introduced to jointly encode geometry and spatially continuous material based on neural fields and volumetric rendering, enabling high-fidelity rendering [1, 16, 21, 27, 44]. Beyond implicit modeling, recent extensions of 3D Gaussian Splatting (3DGS) techniques attach material attributes to Gaussian primitives for fast material reconstruction [9, 20, 25]. While most of these methods require large numbers of samples to optimize material parameters, diffusion-based models can generate new samples for optimization [17, 52] or directly predict high-quality, physically-consistent material maps [4, 23, 26, 31, 48], thereby enhancing reconstruction capabilities, marking a new stage in data-driven material reconstruction.

2.2. Learning-based Material Diffusion

With the advent of deep learning, convolutional and transformer-based networks began predicting material parameters directly from single or multi-view images [8, 22]. Recent advances in diffusion-based generation have produced a diverse set of methods for synthesizing textures and physically based rendering (PBR) materials, yet differences in how multi-view consistency is handled remain a key distinction. In texture generation, most approaches choose to either progressively predict views in sequence—explicitly enforcing cross-view consistency through conditioning [2, 15, 34, 36]—or synthesize all views jointly using cross-attention to ensure coherent global structure [10, 24, 30]. To achieve more realistic rendering effects, recent work leverages similar principles for full PBR material creation: some works adopt a two-stage paradigm, first producing photorealistic renderings through pretrained diffusion models and then recovering material parameters via inverse rendering pipelines [3, 28, 35, 45, 52] or learned prediction networks [14, 51]. While these techniques achieve impressive visual fidelity, most rely on complex multi-stage optimization, which can limit scalability and stability. Other approaches exploit geometric cues and conditions to directly generate multi-view material maps [13, 49]. However, these outputs, although semantically consistent, fail to maintain full fidelity to the conditions. These limitations motivate methods that unify material and texture generation within a high-faithfulness, end-to-end reconstruction framework.



Architecture

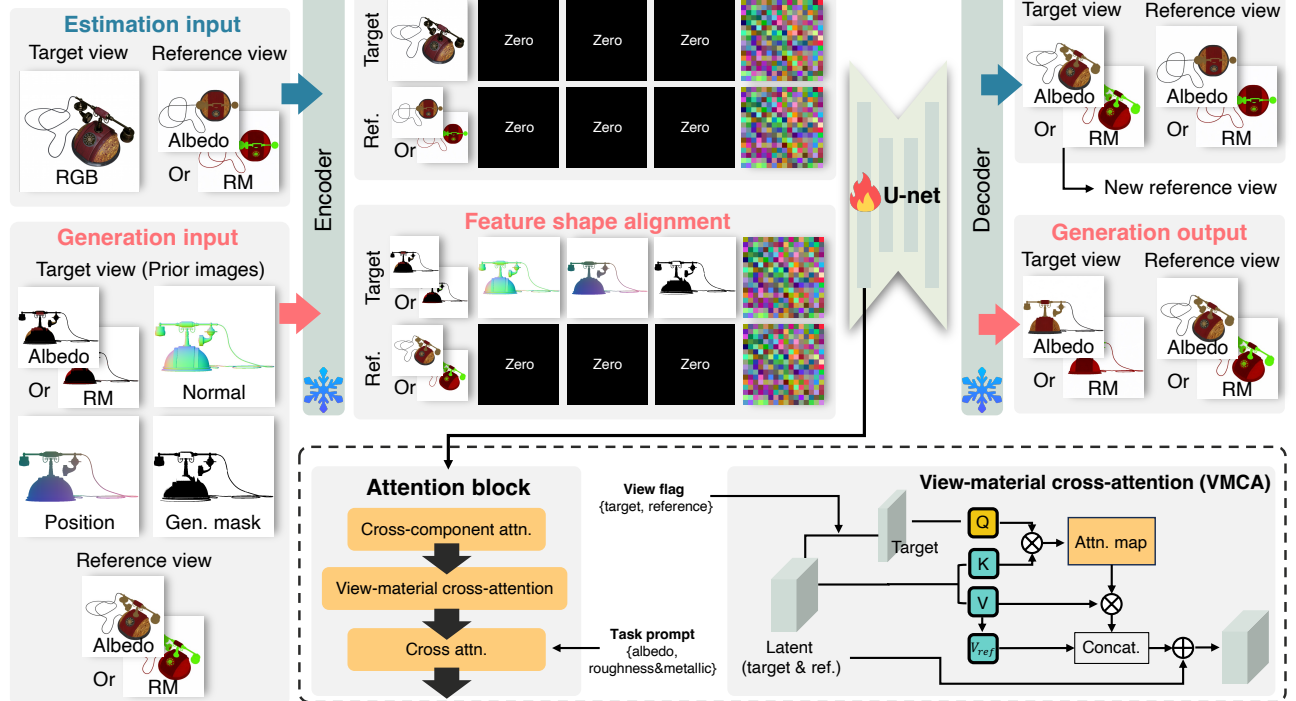


Figure 2. **Method overview.** Our framework, MatMart, divides the material reconstruction task into two stages. In the first stage, progressive material prediction is performed on the input images, and the predicted results are baked into the UV space. In the second stage, prior-guided material generation and texture baking are alternately conducted for unobserved and occluded regions. Both prediction and generation tasks are unified within a single diffusion model and can be accomplished through end-to-end optimization.

3. Method

MatMart is a diffusion-based material reconstruction framework, it aims to reconstruct high-quality PBR materials (*i.e.*, albedo **A**, roughness and metallic **RM**) for 3D objects from input RGB images. As shown in Fig. 2, this framework operates in two main stages. First, we perform progressive inference with the proposed view-material cross-attention to estimate materials for all input images, resulting in globally consistent predictions (Sec. 3.1). Subsequently, we leverage the predicted materials from the first stage as

priors to progressively guide the material generation process (Sec. 3.2). Both prediction and generation tasks are unified within a single diffusion model, and the relevant training and inference details are presented in Sec. 3.3.

3.1. Progressive Material Estimation

Given a set of RGB images, our goal is to estimate their material properties using image-based diffusion and to produce consistent results across the set. However, achieving this with existing techniques [23, 43] presents limitations.

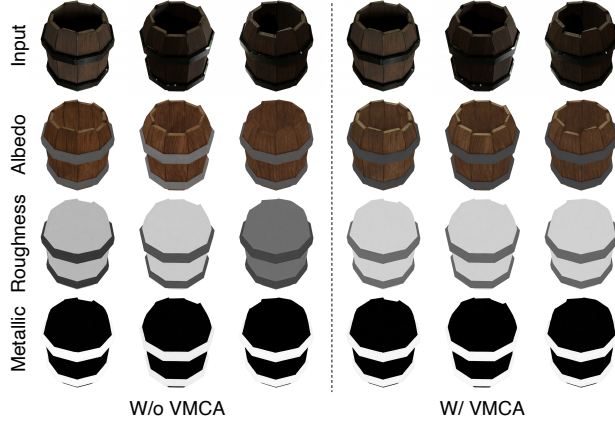


Figure 3. **The effect of VMCA on predicted results.** VMCA improves the consistency for progressive material estimation.

Specifically, to enforce multi-view consistency, these approaches employ cross-view attention, which requires concatenating all input images. This results in a space complexity of $O(N^2)$, which makes it challenging to handle dense or high-resolution inputs, ultimately limiting the scalability and reconstruction quality of the framework. To address this problem, we adopt a progressive inference strategy, sequentially feeding input images into the network for estimation, and propose view-material cross-attention tailored to this process to enforce multi-view consistency.

View-material Cross-attention (VMCA). As progressive inference breaks the information exchange among the inputs, we incorporate a reference view for each inference round. This view is the predicted result from the previous round and serves to establish connections among images inferred in different rounds. Therefore, there are two types of input for each inference: the target view to be estimated, and the reference view containing material information. To build the connection, we perform view-material cross-attention in the latent space between the target view and the reference view, thereby achieving consistent outputs across the views (Fig. 3). This process can be formulated as:

$$\mathbf{Z} = \left(\text{Softmax}\left(\frac{\mathbf{Q}_{\text{Tgt}} \cdot \mathbf{K}_{\text{Tgt+Ref}}^T}{\sqrt{d}}\right) \cdot \mathbf{V}_{\text{Tgt+Ref}} \right) \oplus \mathbf{V}_{\text{Ref}}, \quad (1)$$

where Tgt and Ref denote the indices for the target and reference view, respectively. \mathbf{Q} , \mathbf{K} and \mathbf{V} are the Query, Key and Value features. \oplus denotes concatenation along the sequence dimension, and \mathbf{Z} represents the latent features of target and reference views. As illustrated by Eq. (1), since the reference view is not expected to be influenced by the

target view, it is not used as the Query but is instead directly output as \mathbf{V}_{Ref} . As the numbers of target and reference views are fixed during inference and independent of the total number of input images, the overall space complexity of view-material cross-attention is $O(1)$. This property allows the inference of higher resolutions and an unrestricted number of inputs under limited hardware resources.

3.2. Prior-guided Material Generation

After estimation, all predicted results are baked into UV space. However, in the case of single-view or sparse-view inputs, the baked UV space materials exhibit missing regions in occluded or unobserved parts, and therefore require further completion. Methods such as TEXGen [46] generate materials directly in UV space. We observe that such approaches currently struggle to produce high-quality results (Fig. 5), which may be attributed to the weak semantic information in UV space. Consequently, we opt to generate materials in view space, which has more semantic information. To obtain appropriate viewpoints for generation, we adaptively select views based on geometric information and the texel coverage in UV space. For each selected view, we project the UV space materials into the view space to obtain material priors (*i.e.*, albedo, roughness and metallic). As illustrated in the bottom left of Fig. 2, the material priors contain partial material information, which helps the network generate more consistent results (Fig. 9). For regions requiring generation, we indicate them with a generation mask. In addition, we render geometric priors, including normal and point position, from the known geometry to assist the generation process. These prior images are used as inputs to the network to guide the generation process.

Adaptive View Selection. We select 6 views distributed along the coordinate axes as base views, since they are typically the most informative views. Then, we pick another N views using an adaptive greedy strategy according to the texel coverage, which is obtained by projecting the selected views onto UV space. Specifically, we uniformly sample 300 candidate viewpoints over the sphere and evaluate each of them. In each iteration, the one that yields the maximal improvement in UV space texel coverage is selected. This process is terminated when the target texel coverage ρ is achieved or the number of selected views reaches N . We empirically set $\rho = 0.95$ and $N = 10$. Furthermore, to provide as much material priors as possible for each generation round, we sort the selected $N + 6$ views based on their generation masks. As a result, views containing fewer pixels to be generated are given higher priority for generation.

Alternating Baking and Group-wise Generation. Providing latest material priors for each generation step can

make full use of existing information. Therefore, we perform material generation and baking alternately. The baking process is similar to [40], with modifications to work in a progressive manner. For each generated view space material, we project it onto UV space to obtain a texture map \mathbf{T}' , which is then used to update the existing texture map \mathbf{T} :

$$\mathbf{T} \leftarrow \frac{\mathbf{T}' \cdot \mathbf{W}' + \mathbf{T} \cdot \mathbf{W}}{\mathbf{W}' + \mathbf{W}}, \quad \mathbf{W}' = \mathbf{S}'^\lambda \quad (2)$$

$$\mathbf{W} \leftarrow \mathbf{W}' + \mathbf{W}, \quad (3)$$

where \mathbf{W} and \mathbf{W}' denote the blending weight for texture map \mathbf{T} and \mathbf{T}' respectively. \mathbf{S}' represents the cosine similarity between the normal and the inverse forward axis of camera, which serves to reduce the material contribution at grazing angles. λ is used to modulate the effect of \mathbf{S}' (we follow [40] and set it to 6). For generation, although progressive inference reduces memory consumption, we found that generating for only a single target view at a time is inefficient. Therefore, we choose to infer a group of target views at each step. The group size can be determined according to the memory capacity and GPU utilization (we set it to 3 in our experiments). In most of our experiments, we observe that the choice of group size does not affect the reconstruction quality. Additionally, we use the materials predicted in stage 1 as the reference view and employ VMCA to further enhance the consistency across groups.

Framework Discussion. Considering that Material Anything [14] similarly adopts a progressive generation strategy, we herein discuss the differences. Material Anything employs a pre-trained diffusion model to generate RGB images for all selected views, and then predicts their materials. In contrast, our method first predicts the materials of the input images and subsequently generates materials. Compared to generating RGB images, generating PBR materials is inherently simpler, as it avoids modeling intricate effects such as surface reflections and illumination variations. Our method does not rely on other pre-trained models, thereby avoids the instability introduced by such models. Furthermore, there may be domain differences between the generated RGB data and the training data of the material prediction model, which can reduce the model’s prediction accuracy and ultimately degrade rendering quality (Fig. 5).

3.3. Implementation Details

Unified Architecture. Benefiting from our two-stage framework design that performs material prediction followed by material generation, the outputs of both tasks are unified as PBR materials. And both tasks leverage VMCA to enhance output consistency under progressive inference. These commonalities allow us to integrate both tasks within a unified architecture, thus simplifying the training and deployment process. Specifically, we employ a single diffu-

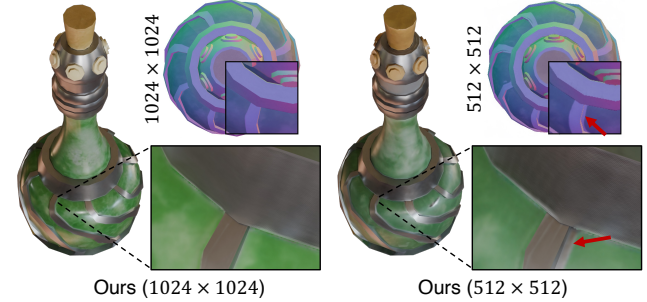


Figure 4. **Generation with high resolution improves texture-geometry alignment.** The top right displays the blended results of normal and generated albedo to visualize the alignment.

sion model, enabling it to have capabilities for both material prediction and generation through end-to-end optimization. To align the shape of input tensors for both tasks, we pad the missing inputs with zeros in feature space. This also serves as an indicator for the model to distinguish between prediction and generation tasks. For the structural details, it is based on a pre-trained Stable Diffusion [37] model. Each attention block consists of three attentions: a cross-component attention for information exchange between \mathbf{A} and \mathbf{RM} , a view-material cross-attention to enhance consistency, and a cross-attention for controlling the type of output materials (\mathbf{A} or \mathbf{RM}) by text prompt.

Training. We alternately optimize our model between the prediction and generation tasks using 16 NVIDIA H20 GPU cards. In each iteration of training, we use two target views and one reference view, where the reference view here is set to the ground truth material. For efficiency, we use depth-based warping to obtain the material priors and generation masks during the optimization of generation task. As the initial view in progressive material estimation does not have a reference view, we additionally include the training for the prediction task without a reference view. The training dataset is the same as that used in IDArb [23], which consists of ABO [5], G-Objaverse [35], and Arb-Objaverse. We start by training for 20K steps on 256×256 images with a batch size of 16, and then further train 50K steps on 512×512 images with a batch size of 4. We use AdamW [29] for optimization, taking v-prediction [38] as the target and assigning a learning rate of 1×10^{-4} .

Inference. The inference of the whole framework is performed on a single V100 GPU card. In both prediction and generation stages, we select the predicted results of the first input image as the reference view. As high resolution improves alignment between geometry and texture in the generated results (Fig. 4), we perform inference at a resolu-

Table 1. Quantitative comparisons for single-view and multi-view settings. Best results are marked as **1st** and **2nd**.

Method	Single-view								Multi-view							
	Albedo		Metallic		Roughness		Rendering		Albedo		Metallic		Roughness		Rendering	
	SSIM↑	PSNR↑	MSE↓	MSE↓	FID↓	LPIPS↓	SSIM↑	PSNR↑	MSE↓	MSE↓	FID↓	LPIPS↓				
NvDiffRec [33]	0.863	25.93	0.059	0.025	73.67	0.145	0.878	26.89	0.066	0.028	60.97	0.117				
Paint3D [47]	0.877	24.66	-	-	60.54	0.166	-	-	-	-	-	-				
Material Anything [14]	0.879	25.97	0.036	0.014	54.16	0.111	0.897	27.19	0.038	0.013	47.27	0.099				
MaterialMVP [13]	0.901	27.57	0.026	0.013	38.27	0.089	0.902	27.61	0.026	0.013	38.00	0.088				
Ours (stage1) + TexGEN [46]	0.908	27.48	-	-	54.10	0.123	0.927	30.23	-	-	47.97	0.102				
Ours (512 × 512)	0.920	28.84	0.025	0.010	31.64	0.076	0.927	29.92	0.022	0.010	31.34	0.068				
Ours (1024 × 1024)	0.931	29.89	0.017	0.007	31.49	0.066	0.945	32.10	0.015	0.008	26.20	0.052				

tion of 1024 in our experiments. During generation, to fully leverage the resolution of each selected view, we adaptively rescale each camera intrinsic by evaluating the projection coverage of geometry surface within the view space, ensuring a high degree of coverage. For meshes without UV mapping, we use Blender’s Smart UV Project to perform the UV unwrapping. For inference at 1024 resolution, reconstructing materials for each object takes around 9 to 23 minutes (depending on the number of selected views N).

4. Experiments

Dataset. For testing, we select a subset of Objaverse [7] comprising 100 objects, and render 9 views of each object with random environment maps. One or three views are used as inputs for single-view and multi-view comparisons, with the remaining views used for evaluation.

Baselines. To evaluate the effectiveness of our method, we select 5 representative approaches as baselines, including Material Anything [14], MaterialMVP [13], Paint3D [47], TexGEN [46], and NvDiffRec [33]. For Material Anything and MaterialMVP, we use our input images as the initial views and conditioning inputs, respectively. Paint3D only works in single-view setting, generating an albedo map conditioned on a single image. TexGEN generates textures conditioned on partial UV space albedo. Since this method is unable to process RGB inputs, we use the predicted albedo of our model (stage1) as its conditioning input. NvDiffRec is an inverse rendering method, we optimize each object using the input images for comparison.

Metrics. To evaluate the accuracy of the reconstructed materials, we compute the scale-invariant Peak Signal-to-Noise Ratio (PSNR) and the Structural Similarity Index Measure (SSIM) [41] for albedo, and the Mean Square Error (MSE) for roughness and metallic. To further assess the fidelity of generation, we calculate the Fréchet Inception Distance (FID) [39] and the Learned Perceptual Image Patch Similarity (LPIPS) [50] on the rendered images.

4.1. Comparisons

We present quantitative comparisons in Tab. 1. Our method achieves more faithful albedo reconstruction, along with more accurate roughness and metallic estimations, resulting in superior FID and LPIPS scores on renderings. When multiple input views are available, the material reconstruction benefits substantially from leveraging the information contained in these views. Our framework is explicitly designed to exploit multi-view inputs, which leads to notable performance gains. Furthermore, higher-resolution inputs enable more precise alignment of fine details, and the substantial improvement in metrics at higher resolutions further validates the effectiveness of our design.

Qualitative comparisons are provided in Fig. 5 and 6, where the ground-truth bump map is applied to all results for better visualization. As an inverse rendering framework, NvDiffRec [33] struggles to disentangle material and illumination with such sparse views, producing noisy renderings under novel illumination. Paint3D [47] produces textures with baked shadows and reflections, as it is not explicitly trained for material prediction. TEXGen [46] leverages our material priors to generate high-quality textures. However, as the UV texture map is produced by the network, its limited resolution results in blurred outputs, such as the textures on the vase. Moreover, generation in the UV space tends to produce noticeable artifacts. For example, the red string on the blue bag is incorrectly generated as another color. MaterialMVP [13] generates visually appealing objects and renderings, but fails to preserve the appearance of the input (such as the icon on the blue bag). In contrast, our method effectively preserves the texture features of the original image. Material Anything [14] also retains original textures by projecting estimated materials into UV space, yet its complex system leads to suboptimal material predictions, as discussed in Sec. 3.2. By end-to-end training the two-stage framework, our method achieves accurate material prediction and consistent material generation, thereby resulting in realistic, semantically coherent outputs.

To further demonstrate the generalizability, we conduct additional experiments on real-world dataset Stanford-

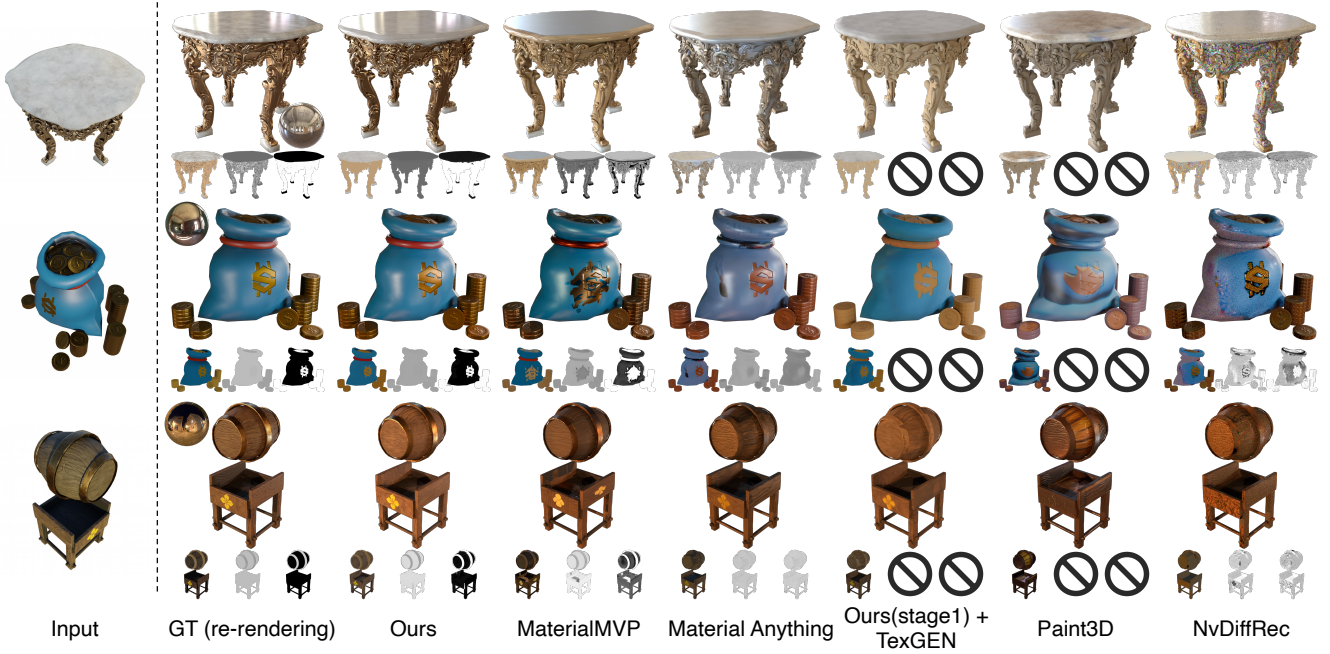


Figure 5. **Qualitative comparison of single-view input.** Our method recovers more accurate materials across various types of objects, thereby achieving rendering results that are more consistent with the ground truth. From left to right are albedo, roughness, and metallic.

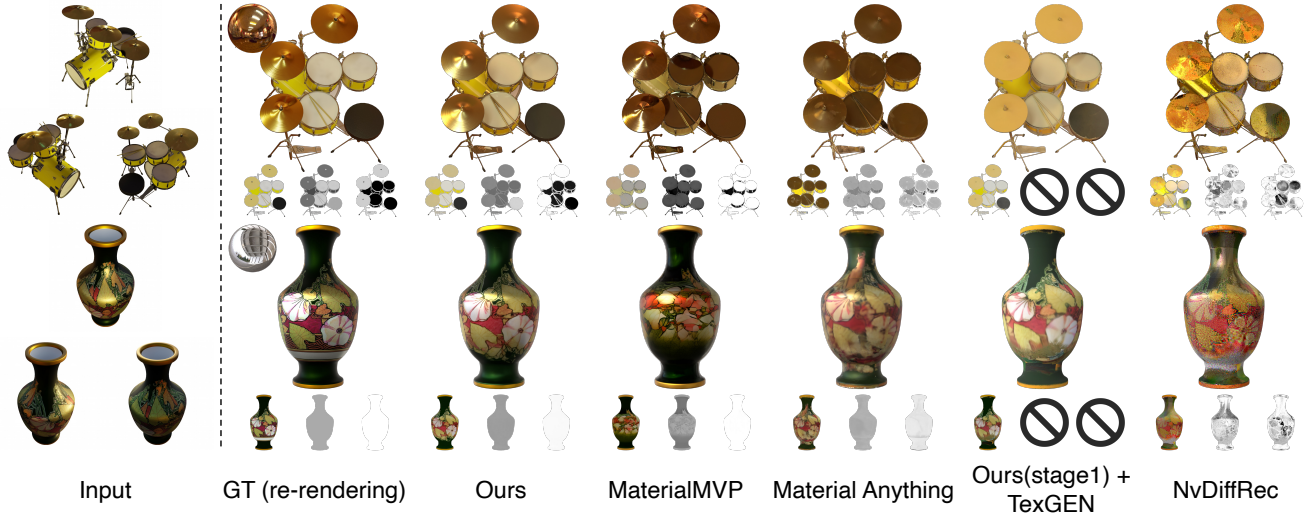


Figure 6. **Qualitative comparison of multi-view input.** Our method recovers consistent materials from multi-view inputs. It preserves the detailed features of the input images, resulting in high-quality renderings. From left to right are albedo, roughness, and metallic.

ORB [19] (Fig. 7). Since most objects in this dataset exhibit strong view-dependent effects, we primarily focus on comparisons with MaterialMVP [13] and Material Anything [14]. Similar to the results of synthetic data, MaterialMVP has difficulty maintaining texture structure, experiencing a loss of semantically meaningful information. Material Anything fails to produce consistent and seamless predictions (such as the seam on the Coke bottle) across

views, especially when handling highly reflective objects, resulting in reduced rendering quality. Compared to these methods, our approach achieves the highest visual fidelity on real-world data, resulting in high-quality renderings.

4.2. Ablation Study

View-material Cross Attention. We validate the effectiveness of VMCA through both quantitative (Tab. 2) and

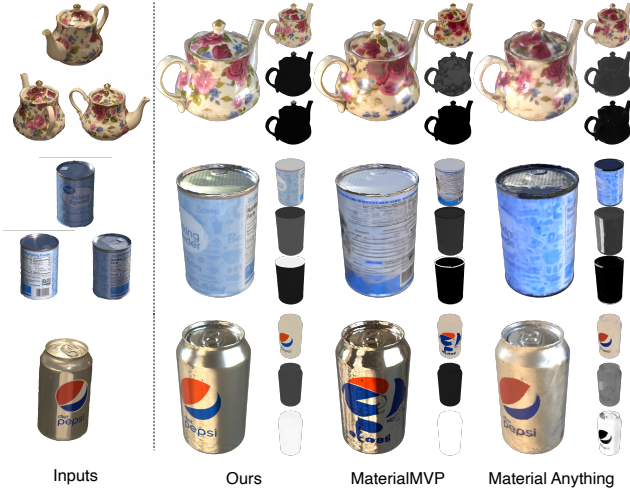


Figure 7. **Qualitative comparison on real-world data Stanford-ORB [19].** From top to bottom: albedo, roughness, and metallic.

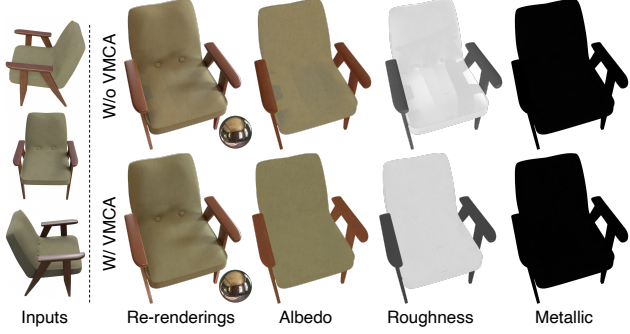


Figure 8. **The effect of VMCA on reconstructed results.** VMCA improves the consistency of reconstructed results.

qualitative comparisons (Fig. 3 and 8). The prediction results shown in the Fig. 3 demonstrate that, without VMCA, the albedo and roughness of the barrel exhibit noticeable inconsistencies. For the final reconstruction, VMCA contributes to greater uniformity in the reconstructed materials, thereby resulting in higher-quality renderings (Fig. 8).

Material Priors. To evaluate the effectiveness of material priors during generation, we fill the material priors with black, thereby avoiding the network accessing any information from them. As shown in Fig. 9, without material priors, the albedo generated based on geometric priors varies across views. These inconsistencies are blended in the same regions of UV space during baking, ultimately resulting in chaotic materials and reduced rendering quality (Tab. 2).

Texture Baking in Stage1. We evaluate the effect of stage1 texture baking on material reconstruction by skip-

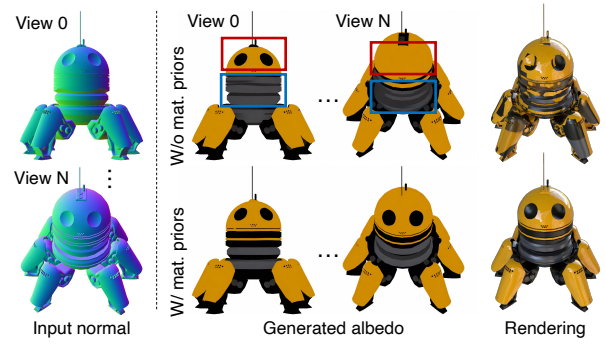


Figure 9. **Material priors ablations.** Material priors ensure the consistency for progressive generation.

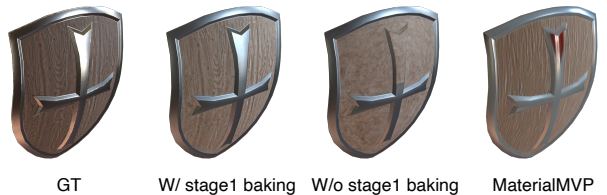


Figure 10. **Stage1 baking improves the quality.**

Table 2. **Ablation study.** Experiments are conducted under a multi-view input setting. Best results are marked as **1st**.

	Albedo		Metallic	Roughness	Rendering	
	SSIM↑	PSNR↑	MSE↓	MSE↓	FID↓	LPIPS↓
W/o VMCA	0.941	31.78	0.016	0.007	28.58	0.055
W/o mat. priors	0.929	29.85	0.018	0.009	34.93	0.071
W/o stage1 baking	0.917	28.14	0.021	0.009	42.40	0.091
Ours (full)	0.945	32.10	0.015	0.008	26.20	0.052

ping this step. In this case, similar to methods like MaterialMVP [13] and Paint3D [47], all materials are obtained through generation. Both quantitative (Tab. 2) and qualitative (Fig. 10) results indicate that achieving high-fidelity materials solely through generation remains a significant challenge. In contrast, generating materials based on the baked textures from stage1 fully leverages prior information, leading to higher-quality reconstructed results.

5. Conclusion

MatMart achieves high-quality material recovery through a two-stage reconstruction approach, making it a practical framework. Compared with other methods, this framework demonstrates high scalability and can be deployed by end-to-end optimization of a single diffusion model. However, as with other material prediction methods, the inherent ambiguity of material decomposition may cause scaled color for the predicted albedo, and objects with strong self-occlusion may require a greater number of views for generation. We leave these limitations for future work.

References

[1] Mark Boss, Raphael Braun, Varun Jampani, Jonathan T Baron, Ce Liu, and Hendrik Lensch. Nerd: Neural reflectance decomposition from image collections. In *Int. Conf. Comput. Vis.*, pages 12684–12694, 2021. 2

[2] Dave Zhenyu Chen, Yawar Siddiqui, Hsin-Ying Lee, Sergey Tulyakov, and Matthias Nießner. Text2tex: Text-driven texture synthesis via diffusion models. In *Int. Conf. Comput. Vis.*, pages 18558–18568, 2023. 2

[3] Rui Chen, Yongwei Chen, Ningxin Jiao, and Kui Jia. Fantasia3d: Disentangling geometry and appearance for high-quality text-to-3d content creation. In *Int. Conf. Comput. Vis.*, pages 22246–22256, 2023. 2

[4] Xi Chen, Sida Peng, Dongchen Yang, Yuan Liu, Bowen Pan, Chengfei Lv, and Xiaowei Zhou. Intrinsicanything: Learning diffusion priors for inverse rendering under unknown illumination. In *Eur. Conf. Comput. Vis.*, pages 450–467. Springer, 2024. 1, 2

[5] Jasmine Collins, Shubham Goel, Kenan Deng, Achleshwar Luthra, Leon Xu, Erhan Gundogdu, Xi Zhang, Tomas F Yago Vicente, Thomas Dideriksen, Himanshu Arora, Matthieu Guillaumin, and Jitendra Malik. Abo: Dataset and benchmarks for real-world 3d object understanding. In *IEEE Conf. Comput. Vis. Pattern Recog.*, 2022. 5

[6] Kristin J Dana, Bram Van Ginneken, Shree K Nayar, and Jan J Koenderink. Reflectance and texture of real-world surfaces. *ACM Trans. Graph.*, 18(1):1–34, 1999. 2

[7] Matt Deitke, Dustin Schwenk, Jordi Salvador, Luca Weihs, Oscar Michel, Eli VanderBilt, Ludwig Schmidt, Kiana Ehsani, Aniruddha Kembhavi, and Ali Farhadi. Objaverse: A universe of annotated 3d objects. *arXiv preprint arXiv:2212.08051*, 2022. 6

[8] Valentin Deschaintre, Miika Aittala, Fredo Durand, George Drettakis, and Adrien Bousseau. Single-image svbrdf capture with a rendering-aware deep network. *ACM Trans. Graph.*, 37(4):1–15, 2018. 2

[9] Kang Du, Zihao Liang, Yulin Shen, and Zeyu Wang. Gs-id: Illumination decomposition on gaussian splatting via adaptive light aggregation and diffusion-guided material priors. In *Int. Conf. Comput. Vis.*, pages 26220–26229, 2025. 2

[10] Yifei Feng, Mingxin Yang, Shuhui Yang, Sheng Zhang, Jia-ao Yu, Zibo Zhao, Yuhong Liu, Jie Jiang, and Chuncho Guo. Romantex: Decoupling 3d-aware rotary positional embedded multi-attention network for texture synthesis. In *Int. Conf. Comput. Vis.*, pages 17203–17213, 2025. 2

[11] Duan Gao, Xiao Li, Yue Dong, Pieter Peers, Kun Xu, and Xin Tong. Deep inverse rendering for high-resolution svbrdf estimation from an arbitrary number of images. *ACM Trans. Graph.*, 38(4):134–1, 2019. 2

[12] Jon Hasselgren, Nikolai Hofmann, and Jacob Munkberg. Shape, light, and material decomposition from images using monte carlo rendering and denoising. *Adv. Neural Inform. Process. Syst.*, 35:22856–22869, 2022. 1, 2

[13] Zebin He, Mingxin Yang, Shuhui Yang, Yixuan Tang, Tao Wang, Kaihao Zhang, Guanying Chen, Yuhong Liu, Jie Jiang, Chuncho Guo, et al. Materialmvp: Illumination-invariant material generation via multi-view pbr diffusion. In *Int. Conf. Comput. Vis.*, 2025. 1, 2, 6, 7, 8

[14] Xin Huang, Tengfei Wang, Ziwei Liu, and Qing Wang. Material anything: Generating materials for any 3d object via diffusion. In *IEEE Conf. Comput. Vis. Pattern Recog.*, pages 26556–26565, 2025. 1, 2, 5, 6, 7

[15] Dong Huo, Zixin Guo, Xinxin Zuo, Zhihao Shi, Juwei Lu, Peng Dai, Songcen Xu, Li Cheng, and Yee-Hong Yang. Texgen: Text-guided 3d texture generation with multi-view sampling and resampling. *Eur. Conf. Comput. Vis.*, 2024. 2

[16] Haian Jin, Isabella Liu, Peijia Xu, Xiaoshuai Zhang, Songfang Han, Sai Bi, Xiaowei Zhou, Zexiang Xu, and Hao Su. Tensoir: Tensorial inverse rendering. In *IEEE Conf. Comput. Vis. Pattern Recog.*, pages 165–174, 2023. 1, 2

[17] Haian Jin, Yuan Li, Fujun Luan, Yuanbo Xiangli, Sai Bi, Kai Zhang, Zexiang Xu, Jin Sun, and Noah Snavely. Neural gaffer: Relighting any object via diffusion. *Adv. Neural Inform. Process. Syst.*, 37:141129–141152, 2024. 2

[18] Peter Kocsis, Vincent Sitzmann, and Matthias Nießner. Intrinsic image diffusion for indoor single-view material estimation. In *IEEE Conf. Comput. Vis. Pattern Recog.*, pages 5198–5208, 2024. 1

[19] Zhengfei Kuang, Yunzhi Zhang, Hong-Xing Yu, Samir Agarwala, Elliott Wu, Jiajun Wu, et al. Stanford-orb: a real-world 3d object inverse rendering benchmark. In *Advances in Neural Information Processing Systems Datasets and Benchmarks Track*, 2023. 7, 8

[20] Shuichang Lai, Letian Huang, Jie Guo, Kai Cheng, Bowen Pan, Xiaoxiao Long, Jiangjing Lyu, Chengfei Lv, and Yanwen Guo. Glossygs: Inverse rendering of glossy objects with 3d gaussian splatting. *IEEE Trans. Vis. Comput. Graph.*, 2025. 2

[21] Jia Li, Lu Wang, Lei Zhang, and Beibei Wang. Tensosdf: Roughness-aware tensorial representation for robust geometry and material reconstruction. *ACM Trans. Graph.*, 43(4):1–13, 2024. 2

[22] Zhengqin Li, Zexiang Xu, Ravi Ramamoorthi, Kalyan Sunkavalli, and Manmohan Chandraker. Learning to reconstruct shape and spatially-varying reflectance from a single image. *ACM Trans. Graph.*, 37(6), 2018. 2

[23] Zhibing Li, Tong Wu, Jing Tan, Mengchen Zhang, Jiaqi Wang, and Dahua Lin. Idarb: Intrinsic decomposition for arbitrary number of input views and illuminations. In *Int. Conf. Learn. Represent.*, 2024. 1, 2, 3, 5

[24] Yixin Liang, Kunming Luo, Xiao Chen, Rui Chen, Hongyu Yan, Weiyu Li, Jiarui Liu, and Ping Tan. Unitex: Universal high fidelity generative texturing for 3d shapes. *arXiv preprint arXiv:2505.23253*, 2025. 2

[25] Zihao Liang, Qi Zhang, Ying Feng, Ying Shan, and Kui Jia. Gs-ir: 3d gaussian splatting for inverse rendering. In *IEEE Conf. Comput. Vis. Pattern Recog.*, pages 21644–21653, 2024. 1, 2

[26] Yehonathan Litman, Or Patashnik, Kangle Deng, Aviral Agrawal, Rushikesh Zawar, Fernando De la Torre, and Shubham Tulsiani. Materialfusion: Enhancing inverse rendering with material diffusion priors. In *2025 International Conference on 3D Vision (3DV)*, pages 802–812. IEEE, 2025. 2

[27] Yuan Liu, Peng Wang, Cheng Lin, Xiaoxiao Long, Jiepeng Wang, Lingjie Liu, Taku Komura, and Wenping Wang. Nero: Neural geometry and brdf reconstruction of reflective objects from multiview images. *ACM Trans. Graph.*, 42(4):1–22, 2023. 2

[28] Zexiang Liu, Yangguang Li, Youtian Lin, Xin Yu, Sida Peng, Yan-Pei Cao, Xiaojuan Qi, Xiaoshui Huang, Ding Liang, and Wanli Ouyang. Unidream: Unifying diffusion priors for relightable text-to-3d generation. In *Eur. Conf. Comput. Vis.*, pages 74–91. Springer, 2024. 2

[29] Ilya Loshchilov and Frank Hutter. Decoupled weight decay regularization. *arXiv preprint arXiv:1711.05101*, 2017. 5

[30] Jiawei Lu, Yingpeng Zhang, Zengjun Zhao, He Wang, Kun Zhou, and Tianjia Shao. Genesistex2: Stable, consistent and high-quality text-to-texture generation. In *AAAI*, pages 5820–5828, 2025. 2

[31] Jundan Luo, Duygu Ceylan, Jae Shin Yoon, Nanxuan Zhao, Julien Philip, Anna Frühstück, Wenbin Li, Christian Richardt, and Tuanfeng Wang. Intrinsicdiffusion: Joint intrinsic layers from latent diffusion models. In *ACM SIGGRAPH 2024 Conference Papers*, pages 1–11, 2024. 1, 2

[32] Wojciech Matusik, Hanspeter Pfister, Matt Brand, and Leonard McMillan. A data-driven reflectance model. *ACM Trans. Graph.*, 22(3):759–769, 2003. 2

[33] Jacob Munkberg, Jon Hasselgren, Tianchang Shen, Jun Gao, Wenzheng Chen, Alex Evans, Thomas Müller, and Sanja Fidler. Extracting Triangular 3D Models, Materials, and Lighting From Images. In *IEEE Conf. Comput. Vis. Pattern Recog.*, pages 8280–8290, 2022. 1, 2, 6

[34] Ben Poole, Ajay Jain, Jonathan T Barron, and Ben Mildenhall. Dreamfusion: Text-to-3d using 2d diffusion. *arXiv preprint arXiv:2209.14988*, 2022. 2

[35] Lingteng Qiu, Guanying Chen, Xiaodong Gu, Qi Zuo, Mutian Xu, Yushuang Wu, Weihao Yuan, Zilong Dong, Liefeng Bo, and Xiaoguang Han. Richdreamer: A generalizable normal-depth diffusion model for detail richness in text-to-3d. In *IEEE Conf. Comput. Vis. Pattern Recog.*, pages 9914–9925, 2024. 2, 5

[36] Elad Richardson, Gal Metzer, Yuval Alaluf, Raja Giryes, and Daniel Cohen-Or. Texture: Text-guided texturing of 3d shapes. In *ACM SIGGRAPH 2023 Conference Papers*, pages 1–11, 2023. 2

[37] Robin Rombach, Andreas Blattmann, Dominik Lorenz, Patrick Esser, and Björn Ommer. High-resolution image synthesis with latent diffusion models. In *IEEE Conf. Comput. Vis. Pattern Recog.*, pages 10684–10695, 2022. 5

[38] Tim Salimans and Jonathan Ho. Progressive distillation for fast sampling of diffusion models. *arXiv preprint arXiv:2202.00512*, 2022. 5

[39] Maximilian Seitzer. pytorch-fid: FID Score for PyTorch. <https://github.com/mseitzer/pytorch-fid>, 2020. Version 0.3.0. 6

[40] Tencent Hunyuan3D Team. Hunyuan3d 2.1: From images to high-fidelity 3d assets with production-ready pbr material. *arXiv preprint arXiv:2506.15442*, 2025. 5

[41] Zhou Wang, A.C. Bovik, H.R. Sheikh, and E.P. Simoncelli. Image quality assessment: from error visibility to structural similarity. *IEEE Trans. Image Process.*, 13(4):600–612, 2004. 6

[42] Gregory J Ward. Measuring and modeling anisotropic reflection. In *Proceedings of the 19th annual conference on Computer graphics and interactive techniques*, pages 265–272, 1992. 2

[43] Xiuchao Wu, Pengfei Zhu, Jiangjing Lyu, Xinguo Liu, Jie Guo, Yanwen Guo, Weiwei Xu, and Chengfei Lyu. Stableintrinsic: Detail-preserving one-step diffusion model for multi-view material estimation. *arXiv preprint arXiv:2508.19789*, 2025. 3

[44] Yao Yao, Jingyang Zhang, Jingbo Liu, Yihang Qu, Tian Fang, David McKinnon, Yanghai Tsin, and Long Quan. Neilf: Neural incident light field for physically-based material estimation. In *Eur. Conf. Comput. Vis.*, pages 700–716. Springer, 2022. 2

[45] Kim Youwang, Tae-Hyun Oh, and Gerard Pons-Moll. Paintit: Text-to-texture synthesis via deep convolutional texture map optimization and physically-based rendering. In *IEEE Conf. Comput. Vis. Pattern Recog.*, pages 4347–4356, 2024. 2

[46] Xin Yu, Ze Yuan, Yuan-Chen Guo, Ying-Tian Liu, Jianhui Liu, Yangguang Li, Yan-Pei Cao, Ding Liang, and Xiaojuan Qi. Texgen: a generative diffusion model for mesh textures. *ACM Trans. Graph.*, 43(6):1–14, 2024. 1, 4, 6

[47] Xianfang Zeng, Xin Chen, Zhongqi Qi, Wen Liu, Zibo Zhao, Zhibin Wang, Bin Fu, Yong Liu, and Gang Yu. Paint3d: Paint anything 3d with lighting-less texture diffusion models. In *IEEE Conf. Comput. Vis. Pattern Recog.*, pages 4252–4262, 2024. 6, 8

[48] Zheng Zeng, Valentin Deschaintre, Iliyan Georgiev, Yannick Hold-Geoffroy, Yiwei Hu, Fujun Luan, Ling-Qi Yan, and Miloš Hašan. Rgb↔x: Image decomposition and synthesis using material- and lighting-aware diffusion models. In *SIGGRAPH2024*, New York, NY, USA, 2024. Association for Computing Machinery. 1, 2

[49] Longwen Zhang, Ziyu Wang, Qixuan Zhang, Qiwei Qiu, Anqi Pang, Haoran Jiang, Wei Yang, Lan Xu, and Jingyi Yu. Clay: A controllable large-scale generative model for creating high-quality 3d assets. *ACM Trans. Graph.*, 43(4):1–20, 2024. 2

[50] Richard Zhang, Phillip Isola, Alexei A Efros, Eli Shechtman, and Oliver Wang. The unreasonable effectiveness of deep features as a perceptual metric. In *IEEE Conf. Comput. Vis. Pattern Recog.*, 2018. 6

[51] Shangzhan Zhang, Sida Peng, Tao Xu, Yuanbo Yang, Tianrun Chen, Nan Xue, Yujun Shen, Hujun Bao, Ruizhen Hu, and Xiaowei Zhou. Mapa: Text-driven photorealistic material painting for 3d shapes. In *ACM SIGGRAPH 2024 Conference Papers*, pages 1–12, 2024. 2

[52] Yuqing Zhang, Yuan Liu, Zhiyu Xie, Lei Yang, Zhongyuan Liu, Mengzhou Yang, Runze Zhang, Qilong Kou, Cheng Lin, Wenping Wang, et al. Dreammat: High-quality pbr material generation with geometry-and light-aware diffusion models. *ACM Trans. Graph.*, 43(4):1–18, 2024. 2